symmetry

MDPI

Article

Research on a Control Strategy of the Symmetrical Four-Roller Bending Process Based on Experiment and Numerical Simulation

Hongqiang Cao [1,2], Gaochao Yu [1,2,*], Chunfang Yang [1,2] and Jun Zhao [1,2]

[1] Key Laboratory of Advanced Forging & Stamping Technology and Science, Yanshan University, Ministry of Education of China, Qinhuangdao 066004, China; frank@ysu.edu.cn (H.C.); cfyang@stumail.ysu.edu.cn (C.Y.); zhaojun@ysu.edu.cn (J.Z.)
[2] College of Mechanical Engineering, Yanshan University, Qinhuangdao 066004, China
* Correspondence: gch_yu@ysu.edu.cn

Abstract: The intelligent production of sheet metal is a comprehensive technology involving control science, computer science, and sheet metal production. Intelligent rolling is an important development in the production process of sheet metal. In this paper, a new symmetrical four-roller bending (SFRB) process is introduced, which consists of feeding, pre-bending, reverse roll bending, second bending, and forward roll bending and unloading. A control strategy is proposed for the process, including on-line monitoring of curvature, on-line identification of the springback law, on-line prediction of final reduction, and control strategy. A convenient and reliable on-line curvature monitoring method is proposed. The quantitative relationship between the reduction and the curvature, in the form of a quadratic function, was established by physical experiments and numerical simulation, and the online identification of the springback law was realized. An on-line prediction method of the final reduction is proposed, and the determination principle of the reduction of three pre-bending processes is given. Finally, the control strategy of the SFRB process was verified by physical experiments. The relative error of the curvature radius of the final formed parts can be controlled within 0.8%. This research provides new insights into intelligent rolling.

Keywords: thin-wall pipes; symmetrical four-roller bending; springback; control strategy

Citation: Cao, H.; Yu, G.; Yang, C.; Zhao, J. Research on a Control Strategy of the Symmetrical Four-Roller Bending Process Based on Experiment and Numerical Simulation. *Symmetry* **2021**, *13*, 940. https://doi.org/10.3390/sym13060940

Academic Editor: Jan Awrejcewicz

Received: 30 April 2021
Accepted: 24 May 2021
Published: 26 May 2021

1. Introduction

The intelligent production of sheet metal is a comprehensive subject that combines control science, computer science, and sheet metal production theory [1]. Intelligent rolling is an important development in the production process of sheet metal. According to the different number of rollers, the roll bending process can be divided into three forms, namely, two-roller, three-roller, and four-roller. In view of different forms of rolling process, scholars have undertaken a significant amount of research on the relationship between the forming curvature and reduction, defect formation, and structural optimization, using theoretical analysis, numerical simulation, and experimental research methods. In the field of three-roller bending, using different methods, Gandhi et al. [2], Zhang et al. [3], Hu and Wang [4], Gandhi et al. [5] and Fu et al. [6], Quan et al. [7], Chudasama et al. [8], and Yu et al. [9,10] constructed mathematical models and obtained theoretical results. Zeng et al. [11], Ktari et al. [12], and Feng et al. [13,14] carried out numerical simulations to obtain the deformation characteristics of the three-roller bending process. Huang et al. [15] presented a new three-roller setting round process to achieve calibration of the roundness of a whole pipe without changing the pipe circumference. In the field of four-roller bending, Hua et al. [16,17], Gao et al. [18], and Sun et al. [19,20] established mathematical models, and Gu et al. [21] developed a finite element model to analyze the four-roll bending process. Yu et al. [22] developed the SFRB process and predicted the reduction of the upper roller; results showed the ovality of the formed part was less than 5%. Li et al. [23] analyzed the

two-roller bending process and established a theoretical model. Gong et al. [24] analyzed the main influencing factors and the distribution of stress and strain.

Because of the simplification of engineering plastic mechanical and material constitutive models, such as the linear kinematic, linear isotropic, and simple kinematic hardening models [9,25,26], it remains a challenge to accurately calculate the reduction according to the target curvature. In production, this mainly depends on the experience of workers and die adjustment, which greatly reduces the production efficiency, and errors are certain to occur. The intelligent control of sheet metal forming is an effective way to address the above problems. Errors caused by theoretical analysis can be compensated for by the monitoring, identification, prediction, and control of the deformation law.

Zhao et al. [1] carried out intelligent drawing of both axisymmetric and non-axisymmetric parts. Li [27] developed an intelligent control system of the JCO forming process for LASW pipes, including theoretical analysis, real-time monitoring of the forming process, identification of material performance parameters, and prediction of process parameters. Zhao et al. [28] developed the control strategy of multi-point bending one-off straightening and control strategy of three-point bending, multi-step straightening. Zhao et al. [29,30] constructed an over-bending setting round intelligent control system for the pipe ends of large pipes, including a pipe-end ovality recognition system, two-step and three-step over-bending setting round control strategy, and real-time prediction of optimum process parameters.

This paper aims to enhance the existing research related to roll bending by proposing the SFRB process. A control strategy is proposed for this process, including on-line monitoring of curvature, on-line identification of the springback law, on-line prediction of the final reduction, and a control strategy process. A convenient and reliable on-line curvature monitoring method is also proposed. The quantitative relationship between the reduction and the curvature was established by physical experiments and numerical simulation, and the online identification of the springback law was realized. An on-line prediction method of the final reduction is also proposed, and the determination principle of the reduction of three pre-bending processes is outlined. Finally, the control strategy of the SFRB process was verified by physical experiments. This research provides new insights into intelligent rolling.

2. SFRB Process

The main working parts of the process are two upper rollers and two lower rollers. The two upper rollers are on the top and active, and the other two rollers are at the bottom and driven. The four rollers are symmetrical along the vertical plane. As shown in Figure 1, the main process includes feeding, pre-bending, reverse roll bending, final bending, positive roll bending, unload, and springback [22]. The process has the advantages of high forming precision, small remaining straight edge, high production efficiency, and simple equipment structure.

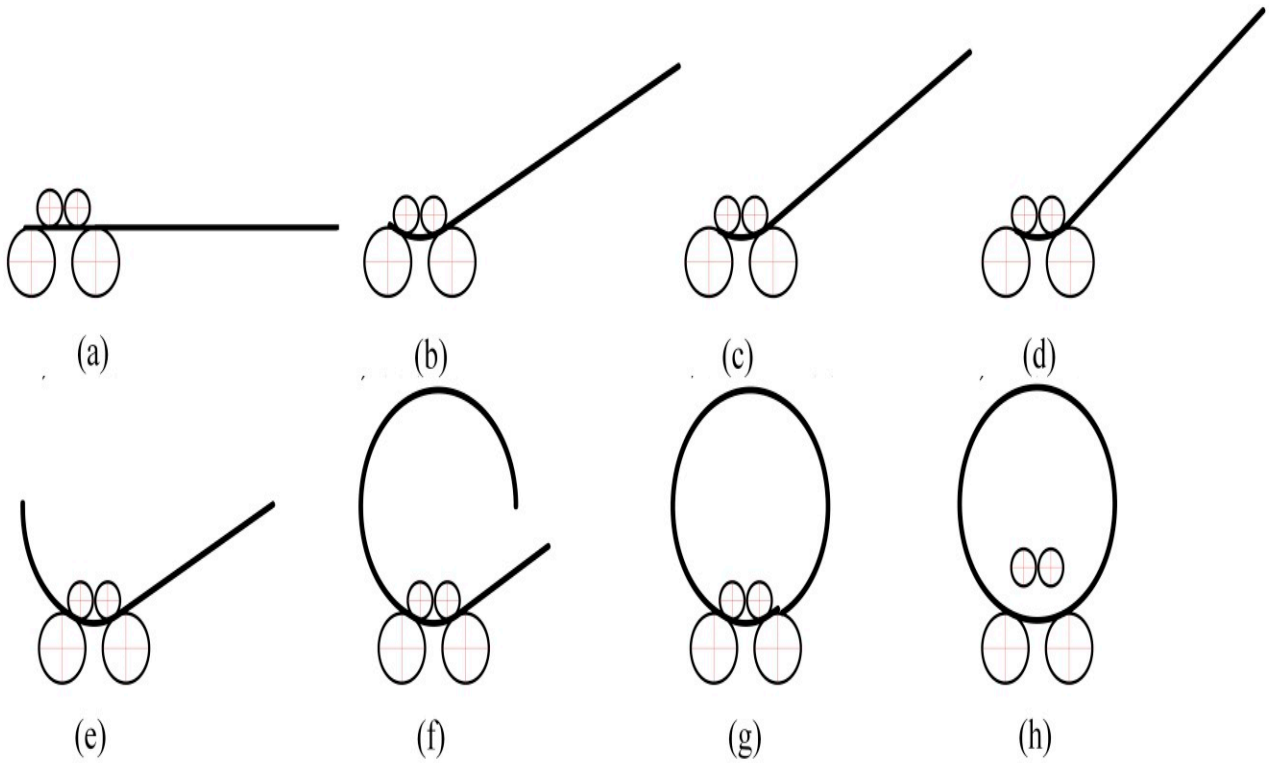

Figure 1. SFRB process: (**a**) feeding, (**b**) pre-bending, (**c**) reverse roll bending, (**d**) final bending, (**e**) positive roll bending, (**f**) positive roll bending, (**g**) bending completion, (**h**) unload and springback.

3. Control Strategy

3.1. Online Monitoring of Curvature

On-line real-time monitoring of the roller bending process can reflect the macroscopic mechanical and geometric parameters of the processed object by adopting effective testing methods. The curvature radius is an important parameter to be monitored online during the roller bending process. At present, in actual production, the method of manual measurement is mostly adopted, which has low efficiency and large error. To realize the purpose of intelligent detection, in this study a new intelligent measurement method was designed. The measuring principle of the method is as follows: after pre-bending or roll bending, the three positions of the formed part are measured, and the curvature radius of the formed part is obtained using the three-point circle principle. The measurement principle is shown in Figure 2.

The measuring point is taken as the coordinate origin, and the direction from the measuring point to position point 1 as the x direction to establish the coordinate system. The coordinates of position No.1, position No.2, and position No.3 are$(\rho_1,\ 0)$, $(\rho_2 \cos\alpha, \rho_2 \sin\alpha)$, and $(\rho_3 \cos(\alpha+\beta), \rho_3 \sin(\alpha+\beta))$. The center coordinate is (x_0, y_0). The coordinates of three positions are brought into the equation of circle:

$$\begin{cases} (\rho_1 - x_0)^2 + (0 - y_0)^2 = r^2 \\ (\rho_2 \cos\alpha - x_0)^2 + (\rho_2 \sin\alpha - y_0)^2 = r^2 \\ (\rho_3 \cos(\alpha+\beta) - x_0)^2 + (\rho_3 \sin(\alpha+\beta) - y_0)^2 = r^2 \end{cases} \quad (1)$$

From Equation (1), the center(x_0, y_0) and curvature radius r can be obtained.

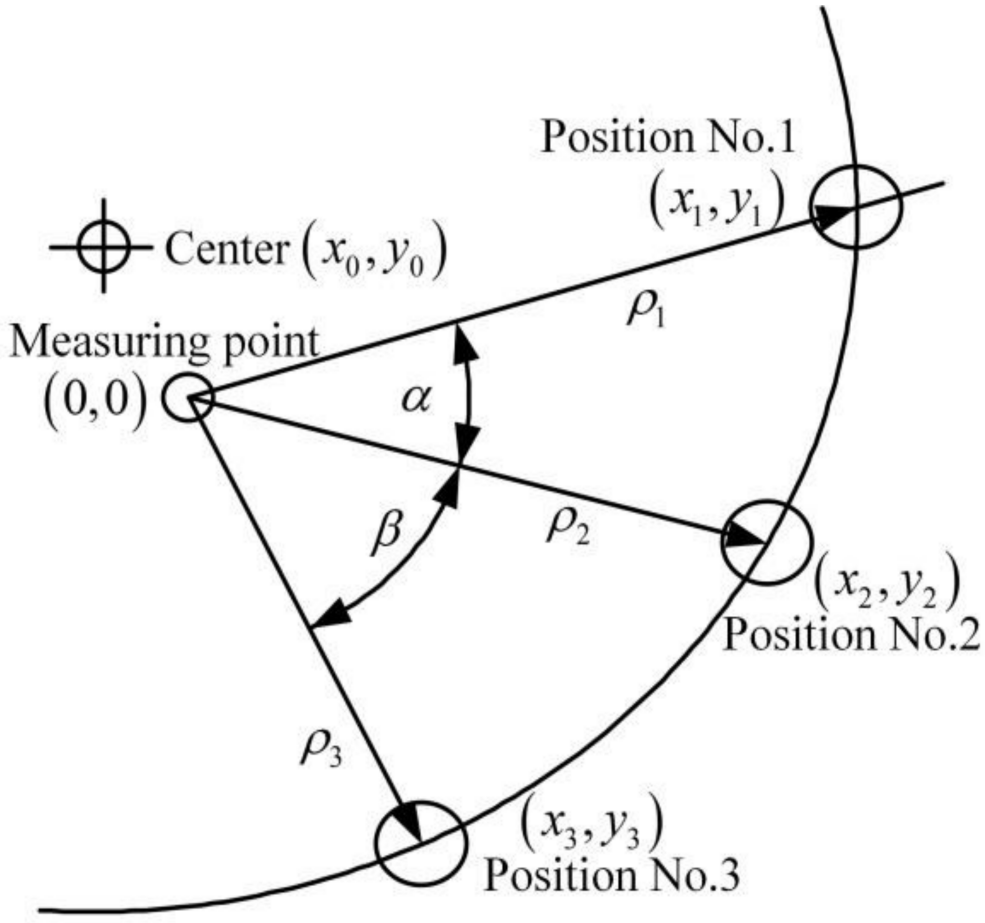

Figure 2. The principle of measuring the curvature radius.

3.2. Online Identification of Springback Law

The quantitative description of the relationship between the upper roller reduction and curvature is the basis of realizing the intelligent control of roll bending. The accuracy of quantitative description determines the identification accuracy and prediction accuracy of the intelligent control system. Based on the monitoring results of curvature, the nonlinear fitting method is adopted to process the results of experiments and numerical simulations, so as to identify the relationship between the reduction and curvature.

3.2.1. Experimental Identification

The SFRB device is shown in Figure 3. The main process parameters of the device are shown in Table 1. ST12 cold-rolled plate and 304 stainless steel, both with 2 mm thickness, were chosen. The relationship between the reduction and curvature was studied using 158, 162, 166, and 168 mm lower roller spacing under different reduction conditions.

Table 1. Main process parameters.

Upper Roller Diameter D_u/mm	Lower Roller Diameter D_1/mm	Upper Roller Spacing L_u/mm	Lower Roller Spacing L_1/mm	Roller Length L_r/mm
60	120	70	150~180	220

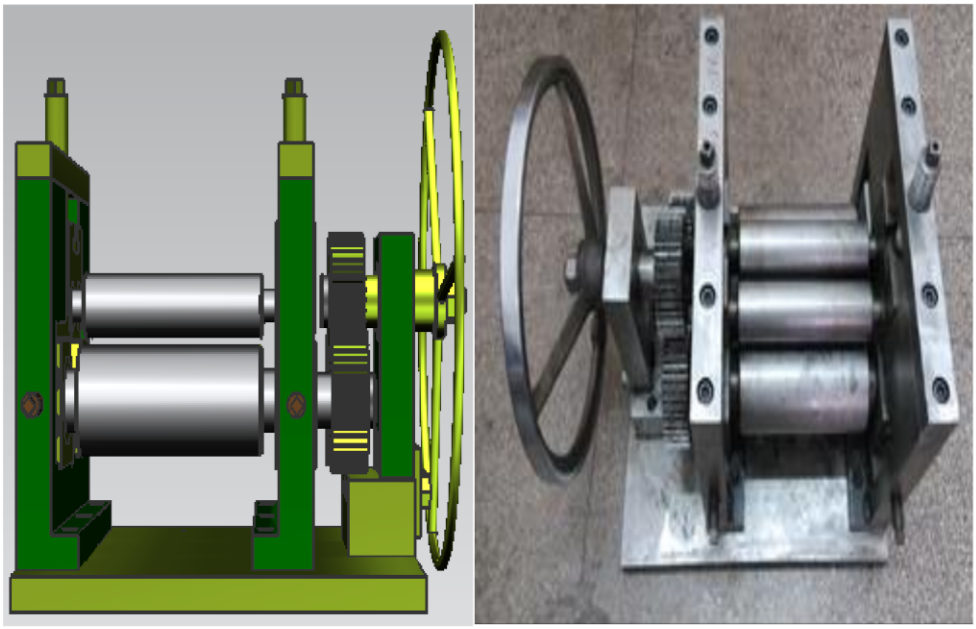

Figure 3. The SFRB device.

When the plate and process conditions are determined, the curvature and reduction are described by Equation (2). The parameters were estimated by the user-defined function equation fitting of Origin Software; the results are shown in Figure 4, and the fitting parameters are shown in Table 2.

$$K(h) = ah^2 + bh + c \tag{2}$$

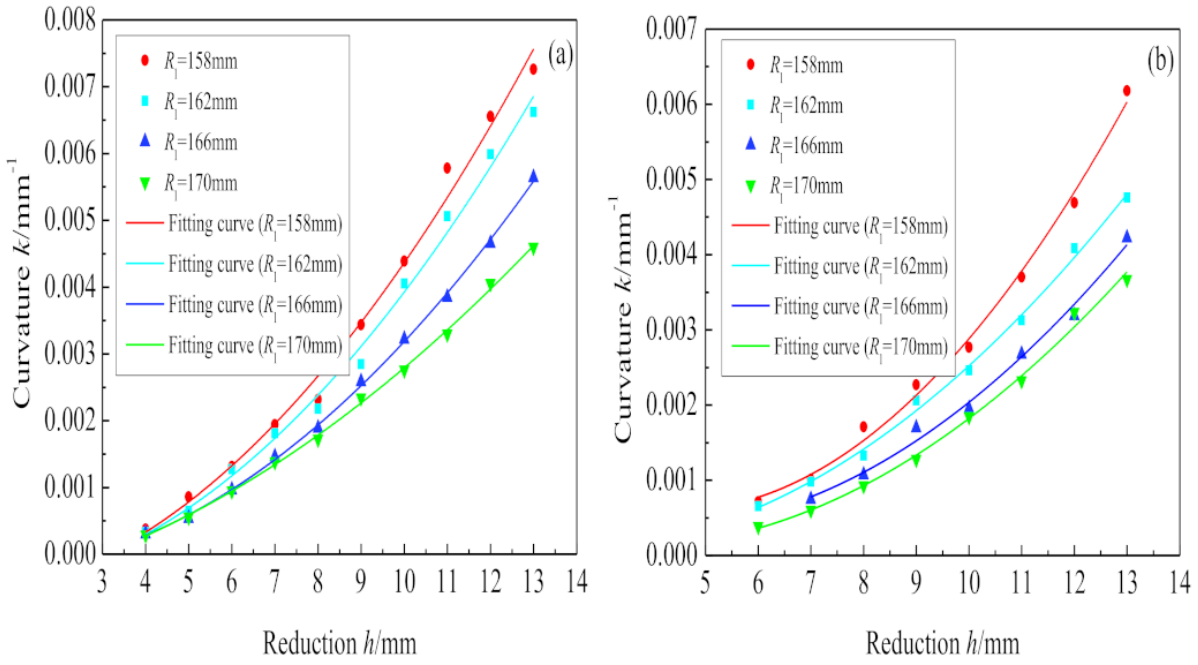

Figure 4. The relationship between the reduction and curvature from experiments: (**a**) ST12 cold rolled plate, (**b**) 304 stainless steel.

Table 2. Fitting parameters from experiments.

Materials	Lower Roller Diameter R_1/mm	a (10^{-6})	b (10^{-6})	C (10^{-6})	R^2
304	158	74.78	−669.38	2100	0.9951
	162	41.58	−194.2	305.59	0.9966
	166	46.63	−373.36	1110	0.9922
	170	40.77	−287.53	619.36	0.9946
ST12	158	43.82	59.00	−606.53	0.9920
	162	41.46	24.55	−465.38	0.9933
	166	35.22	−9.52	−241.73	0.9992
	170	21.22	122.38	−553.51	0.9987

It can be seen from the fitting results that under the condition of keeping the plate and the lower roller spacing unchanged, the relationship between curvature and reduction is a univariate quadratic function. In practical application, this relationship can be used to select the appropriate lower roller spacing and determine the appropriate upper roller reduction.

3.2.2. Numerical Simulation Identification

To increase the accuracy of the research results, the numerical simulation method was used to further verify the relationship between the curvature and reduction. The process parameters of numerical simulations were the same as those of the experiments. The mechanical properties of ST12 cold-rolled plate and 304 stainless steel are shown in Figure 5 and Table 3.

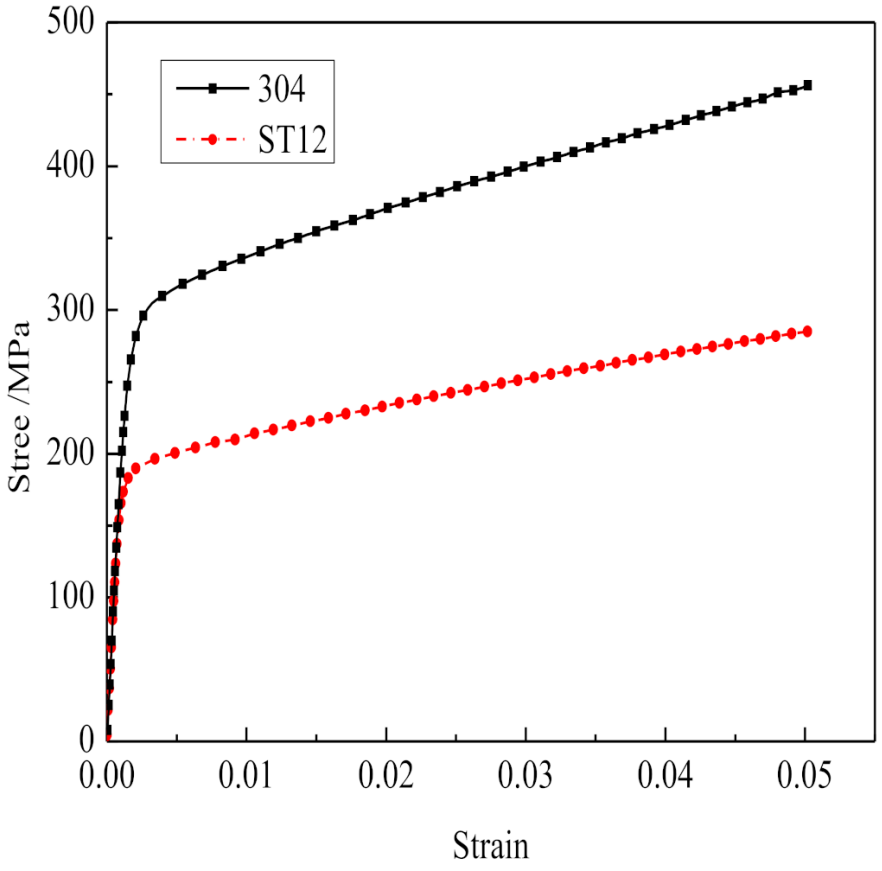

Figure 5. True stress–strain curve.

Table 3. Mechanical properties of pipes.

Materials	Yield Stress/MPa	Young's Modulus/MPa	Plastic Tangent Modulus/MPa
304	257	182,000	2560
ST12	194	202,000	1610

The finite element model of the SFRB process was developed using ABAQUS software, as shown in Figure 6. The two upper rollers and two lower rollers are assumed to be an analytical rigid body. The plate is a deformable body. The master–slave contact condition is set. The frictional coefficient is 0.18. The process was analyzed using the Dynamic/Implicit module.

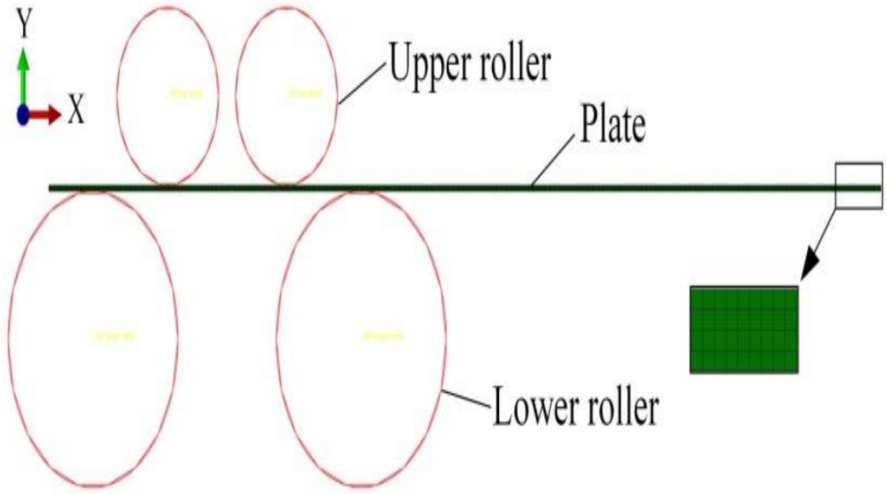

Figure 6. Numerical simulation model.

The relationship between the curvature and reduction and the fitting parameters from the numerical simulation are shown in Figure 7 and Table 4. It can be seen that the relationship between the curvature and reduction still satisfies the one-dimensional quadratic function for ST12 cold rolled plate and 304 stainless steel.

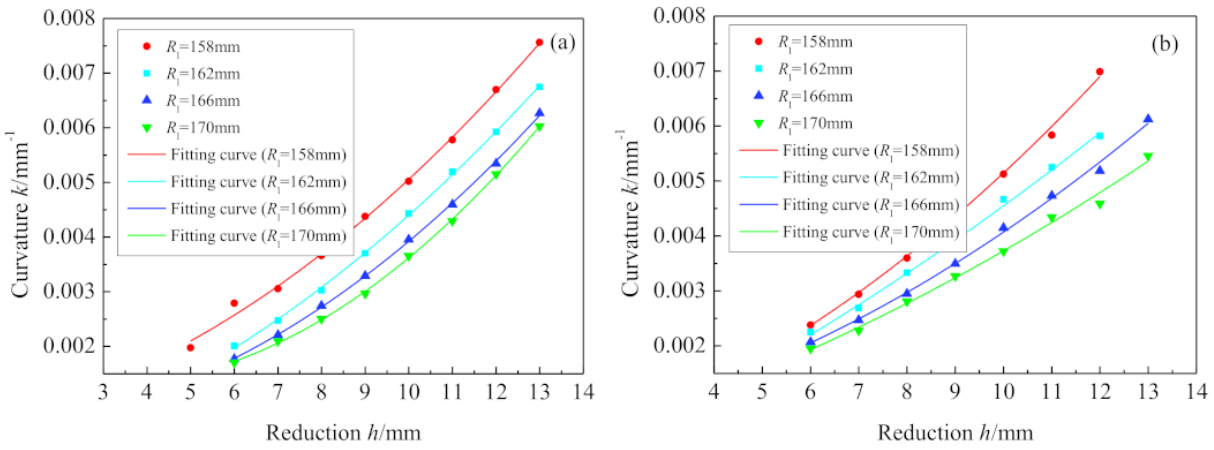

Figure 7. The relationship between the reduction and the curvature from numerical simulations: (**a**) ST12 cold rolled plate, (**b**) 304 stainless steel.

Table 4. Fitting parameters from numerical simulations.

Materials	Lower roller Diameter R_1/mm	a (10^{-6})	b (10^{-6})	c (10^{-6})	R^2
304	158	30.72	202.26	52.28	0.9961
	162	13.13	376.64	−531.6	0.9965
	166	22.31	147.19	367.64	0.9970
	170	13.65	230.74	56.21	0.9936
ST12	158	29.98	141.69	642.76	0.9974
	162	26.03	191.59	−117.48	0.9995
	166	33.16	5.19	556.62	0.9996
	170	46.85	−275.72	1690	0.9996

3.2.3. The Least Square Method

According to the experiments and numerical simulations, the relationship between the curvature and reduction was determined as a univariate quadratic function. To determine the three coefficients in Equation (2), at least three pre-bendings are needed; then, the coefficients of a, b, and c are determined by the least square method. Assuming that the ith reduction corresponding to the curvature k_i, and the total number of reductions is n, then the deviation between the curvature and the function curve can be expressed as:

$$\sum_{i=1}^{n}\left[k_i - (ah_i{}^2 + bh_i + c)\right] \tag{3}$$

The sum of squared residuals is:

$$S = \sum_{i=1}^{n}\left[k_i - \left(ah_i{}^2 + bh_i + c\right)\right]^2 \tag{4}$$

In order to solve the minimum value of S, let:

$$\begin{cases} \frac{\partial M}{\partial a} = 0 \\ \frac{\partial M}{\partial b} = 0 \\ \frac{\partial M}{\partial c} = 0 \end{cases} \tag{5}$$

Then:

$$\begin{cases} a\sum\limits_{i=1}^{n} h_i{}^4 + b\sum\limits_{i=1}^{n} h_i{}^3 + c\sum\limits_{i=1}^{n} h_i{}^2 = \sum\limits_{i=1}^{n} h_i{}^2 k_i \\ a\sum\limits_{i=1}^{n} h_i{}^3 + b\sum\limits_{i=1}^{n} h_i{}^2 + c\sum\limits_{i=1}^{n} h_i = \sum\limits_{i=1}^{n} h_i k_i \\ a\sum\limits_{i=1}^{n} h_i{}^2 + b\sum\limits_{i=1}^{n} h_i + nc = \sum\limits_{i=1}^{n} k_i \end{cases} \tag{6}$$

The three coefficients can be solved using Equation (6).

3.3. Online Prediction of Final Reduction

Considering the actual detection and specific operation, the determination principle of the initial three reductions is as follows: The first reduction h_1 is greater than the elastic limit reduction h_e to ensure plastic deformation. The third reduction h_3 is the reduction when the bending curvature before springback is the target curvature h_t, to ensure that the bending curvature after the three pre-bendings does not exceed the target curvature. The second reduction h_2 is between the first and the third. According to the above principles, the reduction of the first, second, and third pre-bending are, respectively:

$$h_1 = (3h_e + h_t)/4 \tag{7}$$

$$h_2 = (3h_e + 5h_t)/8 \tag{8}$$

$$h_3 = h_t \tag{9}$$

In the rolling process, the maximum strain on the plate section occurs on the outer surface, which can be expressed as:

$$\varepsilon_{out} = \frac{t}{2\rho} \tag{10}$$

where, ε_{out} is the strain of outer surface, t is the thickness, and ρ is the radius of curvature of the neutral layer after deformation.

Let

$$\varepsilon_{out} = \varepsilon_e = \frac{\sigma_s}{E} \tag{11}$$

where ε_e is the elastic limit strain.

Take Equation (10) into Equation (11), and

$$\rho_e = \frac{Et}{2\sigma_s} \tag{12}$$

where ρ_e is the radius of curvature of the neutral layer under the elastic limit condition.

Under the condition of four-point bending, the shape of the plate between the two upper rollers is equal to the curvature arc. Due to the short remaining straight edge in the SFRB process, it is assumed that the shape of the slab between the two lower rollers is also an equal curvature arc under the elastic limit condition. The corresponding center angle is $2\alpha_e$, as shown in Figure 8; then:

$$\sin \alpha_e = \frac{L_l}{2\rho_e + t + 2R_l} \tag{13}$$

where L is the plate length between the two lower rollers.

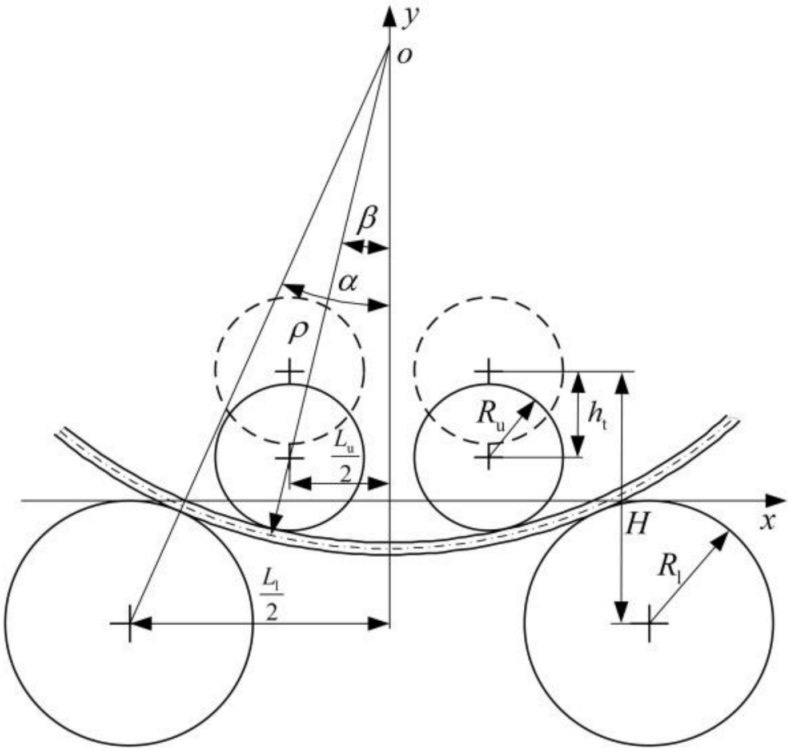

Figure 8. Geometric relationships in the roller bending process.

According to the geometric relationship, there is:

$$h_{\mathrm{e}} = \rho_{\mathrm{e}}(1 - \cos\alpha_{\mathrm{e}}) \tag{14}$$

Substituting Equation (13) into Equation (14), the elastic limit reduction h_e is given by:

$$h_e = \frac{Et}{2\sigma_{\mathrm{s}}}\left(1 - \sqrt{1 - \left(\frac{\sigma_{\mathrm{s}} L_{\mathrm{l}}}{Et + \sigma_{\mathrm{s}} t + 2\sigma_{\mathrm{s}} R_{\mathrm{l}}}\right)^2}\right) \tag{15}$$

When the bending curvature is the target curvature, according to the geometric relationship, h_{t} can be expressed as:

$$h_{\mathrm{t}} = H - (\rho_{\mathrm{t}} + R_{\mathrm{l}} + t/2)\cos\alpha_{\mathrm{t}} + (\rho_{\mathrm{t}} - R_{\mathrm{u}} - t/2)\cos\beta_{\mathrm{t}} \tag{16}$$

$$\alpha_{\mathrm{t}} = \arcsin\frac{L_{\mathrm{l}}}{2\rho_{\mathrm{t}} + t + 2R_{\mathrm{l}}} \tag{17}$$

$$\beta_{\mathrm{t}} = \arcsin\frac{L_{\mathrm{u}}}{2\rho_{\mathrm{t}} - t - 2R_{\mathrm{u}}} \tag{18}$$

where H is the initial vertical distance between upper and lower rollers, ρ_{t} is the target curvature radius.

Through the on-line monitoring of curvature and the online identification of the springback law, the relationship between the reduction and curvature after rolling n times can be obtained, and the final reduction of forming the target curvature can be calculated as:

$$h_{\mathrm{m}} = \frac{\sqrt{b^2 - 4a(c - K_0)} - b}{2a} \tag{19}$$

In production practice, under the condition of a suitable lower roller span, the relationship between the upper roller reduction and curvature can be determined by pre-bending three times. This can be used to predict the upper roller reduction to roll the shape with an arbitrary curvature, which provides a basis for the control strategy of the four-roller bending process.

3.4. Control Strategy Process

According to the three steps of on-line monitoring of curvature, on-line identification of springback law, and on-line prediction of final reduction, the flow chart of the control strategy for the four-roller process was designed as shown in Figure 9.

There are inevitable errors in the measurement after each pre-bending, and the amount of data obtained from pre-bending three times is not enough to accurately fit the curve of the one variable quadratic function of the reduction and the curvature. Therefore, when the curvature of the nth ($n \geq 4$) rolled part fails to meet the accuracy requirements of the target curvature, the results of this rolling can be fed back to the calculation process, the database of relationship of the reduction and curvature can be expanded, and the three coefficients of the quadratic function can be fitted again using the least square method. This further improves the fitting accuracy of the quadratic function until the rolled part meets the accuracy requirements.

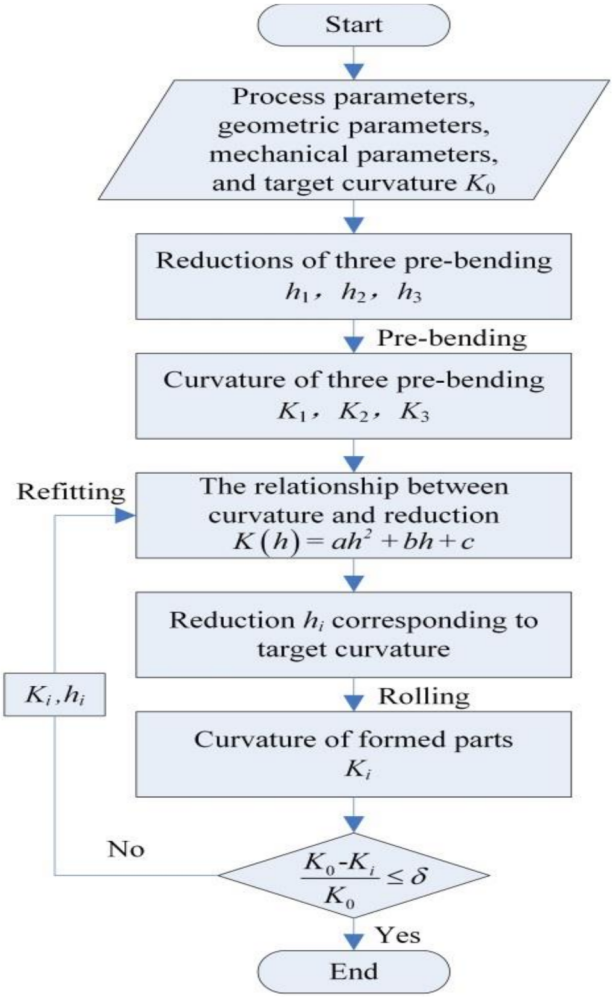

Figure 9. Flowchart of control strategy.

4. Experimental Verification

According to the above-mentioned control strategy and the SFRB device, the ST12 cold rolled plate and 304 stainless steel plate were selected for the verification experiments. The thickness was 2 mm. The three pre-bending processes and the forming part are shown in Figures 10 and 11, respectively. The experimental results are shown in Tables 5 and 6.

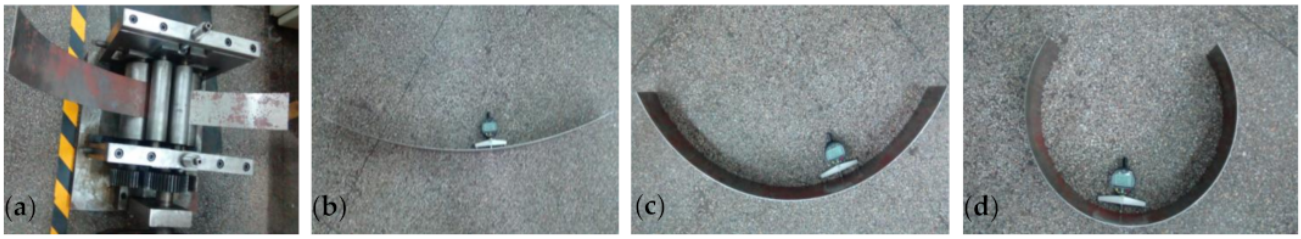

Figure 10. Three pre-bending processes: (**a**) Pre-bending process, (**b**) Plate after pre-bending, (**c**) Plate after second pre-bending, (**d**) Plate after third pre bending.

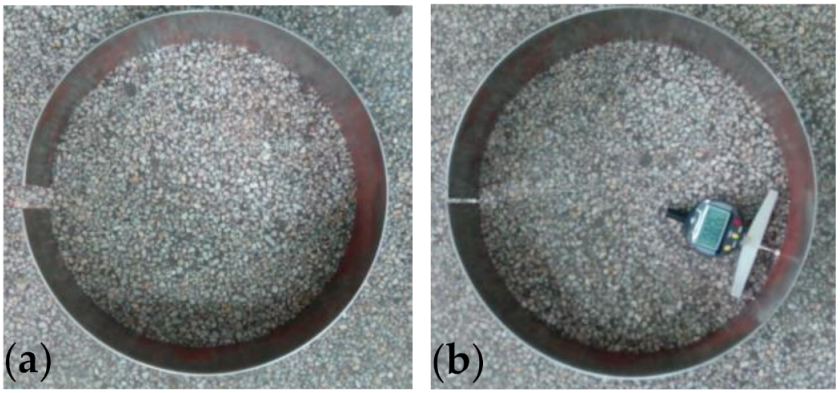

Figure 11. Forming part: (**a**) Before modified rolling, (**b**) After modified rolling.

Table 5. Experimental results for ST12 cold rolled plate (L_1 =163.5 mm).

Procedures	Reduction h/mm	Curvature Radius p /mm	Target Curvature Radius p_t/mm	Error/%
First pre-bending	5.3	1219.5	—	—
Second pre-bending	8.1	436.7		—
Third pre bending	11.2	220.8		—
Rolling	13.2	158.7	150	5.8
Modified rolling	13.4	150.4		0.3

Table 6. Experimental results for 304 stainless steel (L_1 =163.5 mm).

Procedures	Reduction h/mm	Curvature Radius p /mm	Target Curvature Radius p_t/mm	Error/%
First pre-bending	5.8	1762.3	—	—
Second pre-bending	8.5	663.8		—
Third pre bending	11.2	327.2		—
Rolling	14.6	161.2	150	7.5
Modified rolling	14.9	151.1		0.7

It can be seen from Tables 5 and 6 that the curvature radius of the formed part, which is formed by the reduction predicted from three pre-bending processes, has a large error with the target curvature. However, using the above control strategy, the rolling data is substituted into the quadratic function fitting process to obtain the revised reduction. After the modified rolling, the accuracy of the formed parts is clearly improved. The rolling error of the ST12 cold rolled plate is 0.3%, and that of 304 stainless steel plate is 0.7%. Through many experiments, the relative error of the curvature radius of the formed parts is within 0.8%, which verifies the feasibility of the control strategy.

5. Conclusions

In this paper, a new symmetrical four-roller bending process is introduced, which consists of feeding, pre-bending, reverse roll bending, second bending, and forward roll bending and unloading. A control strategy of the SFRB process is also presented based on experiments and numerical simulation. The main conclusions are as follows:

1. For this process, a control strategy is proposed, including on-line monitoring of curvature, on-line identification of the springback law, on-line prediction of final reduction, and control strategy process.

2. A convenient and reliable on-line curvature monitoring method is proposed. The SFRB device was developed and the finite element model was established. Through physical experiments and numerical simulation, the quantitative relationship between the reduction and the curvature was established, which is a quadratic function relationship, as follows:

$$K(h) = ah^2 + bh + c \tag{20}$$

The online identification of the springback law was realized. An on-line prediction method of the final reduction is proposed, and the determination principle of the reduction of three pre-bending processes is given.

3. Through physical experiments, the control strategy of SFRB process was verified. The relative error of curvature radius of the final formed parts can be controlled within 0.8%. This research provides new method for intelligent rolling of steel plate.

Author Contributions: Conceptualization, H.C. and G.Y.; Methodology, H.C. and G.Y.; Software, H.C.; Validation, H.C. and C.Y.; Formal analysis, C.Y.; Writing—original draft preparation, H.C.; Writing—review and editing, G.Y. and J.Z.; Supervision, G.Y.; Funding acquisition, G.Y. All authors have read and agreed to the published version of the manuscript.

Funding: This project was funded and supported by the National Natural Science Foundation of China (52005431), and National Natural Science Foundation of Hebei province (E2020203086).

Institutional Review Board Statement: Not applicable.

Informed Consent Statement: Not applicable.

Data Availability Statement: Not applicable.

Conflicts of Interest: The authors declare no conflict of interest.

References

1. Zhao, J.; Cao, H.Q.; Ma, L.X.; Wang, F.Q.; Li, S.B. Study on intelligent control technology for the deep drawing of an axi-symmetric shell part. *J. Mater. Process Technol.* **2004**, *151*, 98–104. [CrossRef]
2. Gandhi, A.H.; Gajjar, H.V.; Raval, H.K. Mathematical modelling and finite element simulation of pre-bending stage of three-roller plate bending process. *Proc. ASME Int. Manuf. Sci. Eng. Conf.* **2008**, *1*, 617–625. [CrossRef]
3. Zhang, Z.Q.; Song, J.L.; Fu, J.H.; Li, Y.T.; Guo, Y.N. A refined model of three-roller elastoplastic asymmetrical pre-bending of plate. *J. Iron Steel Res. Int.* **2014**, *21*, 328–334. [CrossRef]
4. Hu, W.; Wang, Z.R. Theoretical analysis and experimental study to support the development of a more valuable roll-bending process. *Int. J. Mach. Tool. Manu.* **2001**, *41*, 731–747. [CrossRef]
5. Gandhi, A.H.; Raval, H.K. Analytical and empirical modeling of top roller position for three-roller cylindrical bending of plates and its experimental verification. *J. Mater. Process Technol.* **2008**, *197*, 268–278. [CrossRef]
6. Fu, Z.; Tian, X.; Chen, W.; Hu, B.; Yao, X. Analytical modeling and numerical simulation for three-roll bending forming of sheet metal. *Int. J. Adv. Manuf. Technol.* **2013**, *69*, 1639–1647. [CrossRef]
7. Quan, T.H.; Champliaud, H.; Feng, Z.K.; Salem, J.; My, D.T. Heat-assisted roll-bending process dynamic simulation. *Int. J. Model. Simul.* **2013**, *33*, 54–62. [CrossRef]
8. Chudasama, M.K.; Raval, H.K. Bending force prediction for dynamic roll-bending during 3-roller conical bending process. *J. Manuf. Process.* **2014**, *16*, 284–295. [CrossRef]
9. Yu, G.C.; Zhao, J.; Zhao, F.P. Elastic-plastic secondary indeterminate problem for thin-walled pipe through the inner-wall loading by three-point bending. *Mech. Based. Des. Struc.* **2017**, *45*, 219–238. [CrossRef]
10. Yu, G.C.; Zhao, J.; Zhai, R.X.; Ma, R.; Wang, C.G. Theoretical analysis and experimental investigations on the symmetrical three-roller setting round process. *Int. J. Adv. Manuf. Technol.* **2018**, *94*, 45–56. [CrossRef]
11. Zeng, J.; Liu, Z.; Champliaud, H. FEM dynamic simulation and analysis of the roll-bending process for forming a conical tube. *J. Mater. Process Technol.* **2008**, *198*, 330–343. [CrossRef]
12. Ktari, A.; Antar, Z.; Haddar, N. Modeling and computation of the three-roller bending process of steel sheets. *J. Mech. Sci. Technol.* **2012**, *26*, 123–128. [CrossRef]
13. Feng, Z.K.; Champliaud, H.; Dao, T.M. Numerical study of non-kinematical conical bending with cylindrical rolls. *Simul. Model. Pract. Theory* **2009**, *17*, 1710–1722. [CrossRef]
14. Salem, J.; Champliaud, H.; Feng, Z.K.; Dao, T.M. Experimental analysis of an asymmetrical three-roll bending process. *Int. J. Adv. Manuf. Technol.* **2016**, *83*, 1823–1833. [CrossRef]

15. Huang, X.Y.; Yu, G.C.; Zhao, J.; Mu, Z.K.; Zhang, Z.Y.; Ma, R. Numerical simulation and experimental investigations on a three-roller setting round process for thin-walled pipes. *Int. J. Adv. Manuf. Technol.* **2020**, *107*, 355–369. [CrossRef]
16. Hua, M.; Baines, K.; Cole, I.M. Bending mechanisms, experimental techniques and preliminary tests for the continuous four-roll plate bending process. *J. Mater. Process Technol.* **1995**, *48*, 159–172. [CrossRef]
17. Hua, M.; Lin, Y.H. Large deflection analysis of elastoplastic plate in steady continuous four-roll bending process. *Int. J. Mech. Sci.* **1999**, *41*, 1461–1483. [CrossRef]
18. Gao, G.Y.; Yu, G.C.; Zhao, J.; Zhang, Z.Y. Rolling round process of four-roll and its springback analysis. *J. Plast. Eng.* **2017**, *24*, 55–62.
19. Wu, K.; Sun, Y.; Cao, C.; Zhou, C.; Liu, Q.; Chang, X. On simulation analysis of plate forming and deformation compensation technology of the side roll for four-roll plate bending machine. *Procedia Eng.* **2017**, *207*, 1617–1622. [CrossRef]
20. Zhou, C.; Sun, Y.; Wu, K.; Liu, Q.Y.; Chang, X.; Sheng, Y.L. Modeling and analysis of process parameters in multi-pass four-roll bending. *J. Plast. Eng.* **2018**, *25*, 35–41.
21. Gu, X.; Franzke, M.; Bambach, M.; Hirt, G. Experimental and numerical investigation of grid sheet bending behavior in four-roll bending. *CIRP Ann. Manuf. Technol.* **2010**, *59*, 303–306. [CrossRef]
22. Yu, G.C.; Zhao, J.; Xu, C.F. Development of a symmetrical four-roller bending process. *Int. J. Adv. Manuf. Technol.* **2019**, *104*, 4049–4061. [CrossRef]
23. Li, J.; Li, X.F.; Chen, G.Y.; Zuo, D.W.; Sun, Y.B.; Li, M.; Zhu, C.F. Experiment and simulation of two-axle bending of 301 stainless steel strip with different hardness values. *J. Plast. Eng.* **2017**, *24*, 28–32.
24. Gong, J.P.; Li, X.F.; Zuo, D.W.; Kang, X.J.; Qiu, J.B. Three-dimensional FEA of manufacturing process of small-diameter split sleeve by two-axle bending. *China Mech. Eng.* **2015**, *26*, 1117–1124.
25. Zhao, J.; Yu, G.C.; Ma, R. A mechanical model of symmetrical three-roller setting round process: The static bending stage. *J. Mater. Process Technol.* **2016**, *231*, 501–512. [CrossRef]
26. Yu, G.C.; Zhai, R.X.; Zhao, J.; Ma, R. Theoretical analysis and numerical simulation on the process mechanism of two-roller straightening. *Int. J. Adv. Manuf. Technol.* **2018**, *9*, 4011–4021. [CrossRef]
27. Li, J. *Research on Intelligent Control Technology for Forming the Large Diameter Longitudinal-Seam Submerged ARC Welded Pipes with JCO Process*; Yanshan University: Qinhuangdao, China, 2009.
28. Zhao, J.; Song, X.K. Control strategy of multi-point bending one-off straightening process for LSAW pipes. *Int. J. Adv. Manuf. Technol.* **2014**, *72*, 1615–1624. [CrossRef]
29. Zhao, J.; Zhan, P.P.; Ma, R.; Zhai, R.X. Control strategy of over-bending setting round for pipe-end of large pipes by mould press type method. *Trans. Nonferr. Metal. Soc.* **2012**, *22*, 329–334. [CrossRef]
30. Zhao, J.; Zhan, P.P.; Ma, R.; Zhai, R.X. Prediction and control of springback in setting round process for pipe-end of large pipe. *Int. J. Pres. Ves. Pip.* **2014**, *116*, 56–64. [CrossRef]